AIP Applied Physics Letters

Tunable linear magnetoresistance in MgO magnetic tunnel junction sensors using two pinned CoFeB electrodes

J. Y. Chen, J. F. Feng, and J. M. D. Coey

Citation: Applied Physics Letters **100**, 142407 (2012); doi: 10.1063/1.3701277
View online: http://dx.doi.org/10.1063/1.3701277
View Table of Contents: http://scitation.aip.org/content/aip/journal/apl/100/14?ver=pdfcov
Published by the AIP Publishing

Tunable linear magnetoresistance in MgO magnetic tunnel junction sensors using two pinned CoFeB electrodes

J. Y. Chen,[a] J. F. Feng, and J. M. D. Coey[b]
School of Physics and CRANN, Trinity College, Dublin 2, Ireland

(Received 22 December 2011; accepted 17 March 2012; published online 4 April 2012)

MgO-barrier magnetic tunnel junction sensors with both CoFeB layers pinned by IrMn have been fabricated, which show a tunneling magnetoresistance (TMR) of up to 255% at room temperature. The perpendicular configuration for magnetic field sensing is set using a two-step field annealing process. The linear TMR field range and sensitivity are tuned by inserting an ultrathin Ru layer between the upper IrMn and the top-pinned CoFeB layer. The field sensitivity reaches 26%/mT, while the noise detectivity is about 90 nT/$\sqrt{Hz}$ at 10 Hz for a 0.3 nm Ru insertion layer. The bias dependence of the noise suggests that this is a useful design for sensor applications. © *2012 American Institute of Physics*. [http://dx.doi.org/10.1063/1.3701277]

Magnetic tunnel junctions (MTJs) with a crystalline MgO barrier have been very extensively studied in recent years. Following theoretical predictions,[1,2] a tunnel magnetoresistance (TMR) ratio up to 200% was achieved in MgO MTJs.[3,4] TMR as large as 600% at room temperature has been reported in pseudo spin valve stacks,[5] which is approaching the theoretical maximum.[1,2] Major advances in MgO-barrier MTJs have made them excellent candidates for spin electronic devices, such as spin-torque magnetic random access memory (ST-MRAM),[6] magnetic field sensors,[7] or logic devices.[8] For the magnetic field sensing applications, the stacks are usually configured so that the magnetization of the free layer is perpendicular to that of the pinned layer. When applying a magnetic field along the hard axis of free layer, the magnetization of free layer rotates coherently, which leads to a linear and hysteresis-free response in the magnetoresistance curve. To obtain such a configuration, either high shape anisotropy[9] or a magnetic bias field[10] is often used in sensor devices. However, these configurations require a complicated design and only show a linear response over a small field range, which may not be sufficient for some applications.

Recently, Negulescu *et al.*[11] reported an MTJ sensor device with an Al_2O_3 tunnel barrier using two exchange pinned electrodes, which improves the linear field range, but with a relatively small TMR and a low sensitivity. Good sensors should possess wide operating field range, as well as high field sensitivity and low noise detectivity. In this letter, we demonstrate a type of MTJ sensor with an MgO-barrier, which has these characteristics. The parameters can be tuned by varying the exchange coupling by inserting less than a monolayer of Ru between the top CoFeB layer and its IrMn pinning layer. Furthermore, the ultra-thin Ru increases the TMR in our MTJs and makes the bias-dependence more symmetric. The bias dependence of low frequency noise of these sensors is also discussed.

The MgO-based MTJ stacks with a layer sequence Ta 5/Ru 30/Ta 5/$Ni_{81}Fe_{19}$ (NiFe) 5/$Ir_{22}Mn_{78}$ (IrMn) 10/Co_{90} Fe_{10} 2.5/Ru 0.9/Co_{40} Fe_{40} B_{20} (CoFeB) 3/MgO 2.5/CoFeB 3/Ru (t_{Ru})/IrMn 6/NiFe 5/Ta 5/Ru 5 (thicknesses in nanometers) were deposited onto a thermally oxidized silicon wafer at room temperature. All metallic multilayers were grown by dc-magnetron sputtering, and the MgO layers were grown by rf-sputtering from two MgO targets in a target-facing-target gun in a Shamrock sputtering tool. The thin Ru layer was inserted between the top CoFeB layer and IrMn in order to modulate the exchange coupling between them. The Ru layer thickness used was $t_{Ru} \sim 0$, 0.1, 0.2, or 0.3 nm. Different thicknesses of IrMn were chosen for the top and bottom exchange bias layers in order to modify their thermal stability. The blocking temperature of the IrMn layer depends on its thickness as well as its position in the stack.[11,12] Here NiFe is used to induce a well crystallized IrMn bottom layer.[13] All MTJs were patterned by UV lithography and Ar ion milling to give circular (4 μm in diameter) or rectangular-shaped ($4 \times 12\ \mu m^2$) junctions. The experimental results show almost no difference between two shapes of MTJs because of the weak pinning of the top CoFeB, and all data shown below are for circular junctions. The resistance-area (RA) product of the MTJs selected in this study ranged from $50 \sim 100\ k\Omega\ \mu m^2$. High vacuum post-annealing was performed at 350 °C (first anneal) and 150 °C (second anneal) in an applied magnetic field of 800 mT for 1 h. The first annealing step at high temperature initializes both top and bottom pinned layers in the same direction as well as inducing the crystallization of CoFeB and MgO required for high TMR. The second annealing step at 150 °C with the applied magnetic field perpendicular to the first field direction aims to set an orthogonal configuration for the top layer. Both magnetotransport and noise measurements were performed by a four-probe method at room temperature. Positive bias is defined as the direction of electron flow from the top to the bottom CoFeB electrodes.

Figure 1(a) show the typical TMR major loops after the first anneal at 350 °C and after the second anneal at 150 °C for the same MTJ with $t_{Ru} = 0.1$ nm. The M-H loop for unpatterned MTJ stacks was also measured, as shown in Fig. 1(b), which shows the independent rotation of top-pinned CoFeB, NiFe, and the bottom-pinned synthetic antiferromagnetic (SAF) $Co_{90}Fe_{10}$/Ru/CoFeB layers. The SAF stack

[a]Electronic mail: chenju@tcd.ie.
[b]Electronic mail: jcoey@tcd.ie.

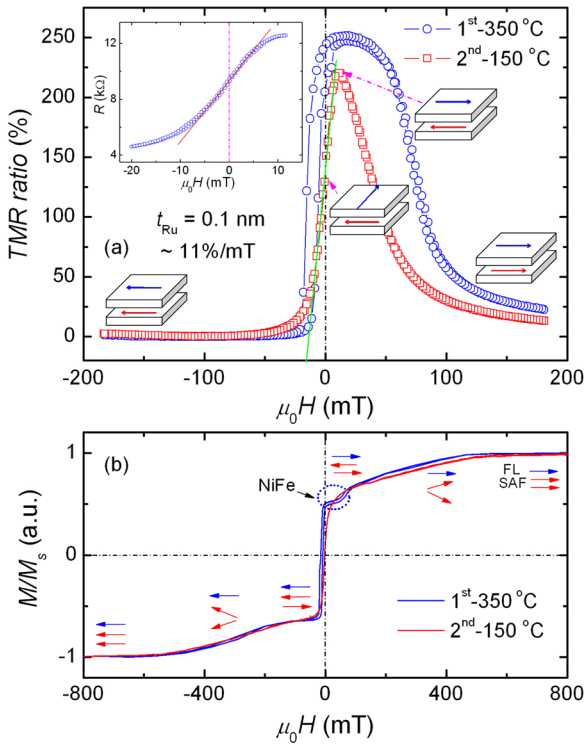

FIG. 1. (a) Typical TMR curves and (b) M-H loops measured along the easy axis of the bottom pinned layer after the first annealing step at 350 °C and the second annealing step at 150 °C for $t_{Ru} = 0.1$ nm. The inset of (a) shows the transverse curve in a small field range. The small cartoons show the magnetic configuration of two layers after the second anneal.

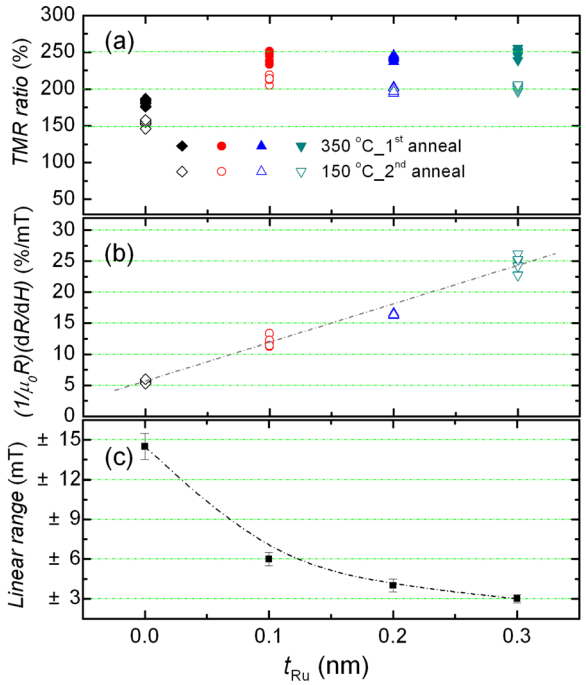

FIG. 2. (a) TMR after first and second anneal, (b) the field sensitivity and (c) linear field range as a function of Ru inserting layer thickness (t_{Ru}). The dashed lines are guide to the eyes.

shows a spin flop configuration during the magnetization rotation. When the orthogonal configuration forms after the second anneal, the magnetization switching of NiFe becomes weak. In the low-field range, only the magnetization of the top-pinned CoFeB layer switches. A TMR ratio of 254% was obtained in this junction, which confirms the high quality of MgO and CoFeB. The TMR curve after the first annealing step at 350 °C has an obvious shift to negative fields, which corresponds to the exchange coupling field (H_{ex}) for the top pinned layers CoFeB 3/Ru ($t_{Ru} = 0.1$)/IrMn 6: $\mu_0 H_{ex} = 9.9$ mT. As t_{Ru} increases from 0 to 0.3 nm, $\mu_0 H_{ex}$ decreases exponentially from 15.4 to 2.0 mT. After the second annealing step at 150 °C, the top pinned CoFeB layer was set in a direction orthogonal to the first annealing direction. This anneal did not greatly affect the orientation of the bottom-pinned layers IrMn/$Co_{90}Fe_{10}$/Ru/CoFeB due to high thermal stability of the 10 nm IrMn pinning. The TMR was measured with the applied field along the original bottom-pinned layer direction, and an obvious linear response is obtained with a TMR ratio of 219%. It can be improved up to 250% by changing the applied field direction by 30°.

Figure 2(a) summarizes the TMR ratios for several junctions against t_{Ru}. Without inserting Ru, IrMn directly adjacent to the top CoFeB layer, gives strong exchange coupling after the first anneal. The TMR ratio is about 160%. The capping layer on top of the upper CoFeB electrode was found to have a strong influence on the crystallization of CoFeB.[14–16] For example, Yuasa *et al.*[14] reported that an fcc (111) NiFe cap layer will induce the same (unwelcome) texture in CoFeB after annealing. In our case, the influence of IrMn on the crystallization of top CoFeB electrode is modified by the Ru dusting layer. On inserting only 0.1 nm of Ru, the TMR ratio increases up to 255%, the bias dependence becomes more symmetric and the noise is reduced, all of which suggest that the Ru helps the top CoFeB electrode to crystallize with the required bcc (001) texture. After the second anneal, the TMR ratio and the exchange bias due to the bottom IrMn are diminished (Figs. 1 and 2(a)). This is because the magnetization direction of the bottom-pinned electrodes is altered by about 30° after the second anneal so that the top and bottom CoFeB layer are not precisely orthogonal. The field sensitivity ($s = (1/\mu_0 R)(\mathrm{d}\,R/\mathrm{d}\,H)$) of several junctions varies as a function of t_{Ru} as plotted in Figure 2(b). Without inserting the Ru layer, s is only about 5%–6%/mT. However, when the Ru layer was inserted, the s value increases almost linearly with t_{Ru}, up to 26%/mT at $t_{Ru} = 0.3$ nm. Our results give evidence that the field sensitivity of these MTJ sensors is inversely proportional to H_{ex}.[17] On further increasing t_{Ru}, no further improvement was found due to sharply weakened exchange coupling, and it is hard to form the orthogonal configuration. As t_{Ru} increases, the linear field range is tunable and decreases monotonically from ±15 mT at $t_{Ru} = 0$ nm to ±3 mT at $t_{Ru} = 0.3$ nm, as shown in Figure 2(c). The linear field range is changed by a factor of five, which is similar to that reported by Negulescu *et al.*[11] for their Al_2O_3 barrier, but a higher field sensitivity can be obtained in our sensors due to the larger TMR effect with the MgO barrier.

Figure 3(a) presents the normalized noise parameter α and TMR as a function of applied magnetic field with an applied bias voltage of 10–30 mV. The thermal noise and amplifier noise have been subtracted. Both junction resistance and the noise power spectrum centered at 4.8 Hz are measured simultaneously at a constant current. The inset gives the noise power spectral density as a function of frequency in different states, which shows 1/*f* noise. Usually, the 1/*f* noise of MTJs can be

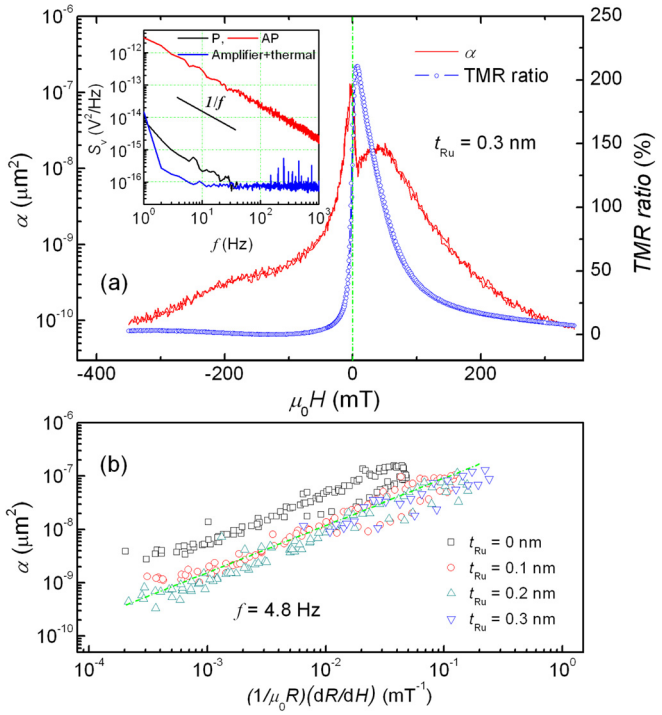

FIG. 3. (a) The magnetic field dependence of Hooge-like parameter (α) and TMR ratio for an MTJ with $t_{Ru} = 0.3$ nm. The inset shows the $1/f$ noise power spectral density as a function of frequency in the parallel (−300 mT) and antiparallel states (6.5 mT) after subtracting the thermal and amplifier noise. (b) α during magnetization switching of top-pinned CoFeB layer plotted against field sensitivity for different t_{Ru}. The dashed line has unit slop and is a guide to the eye.

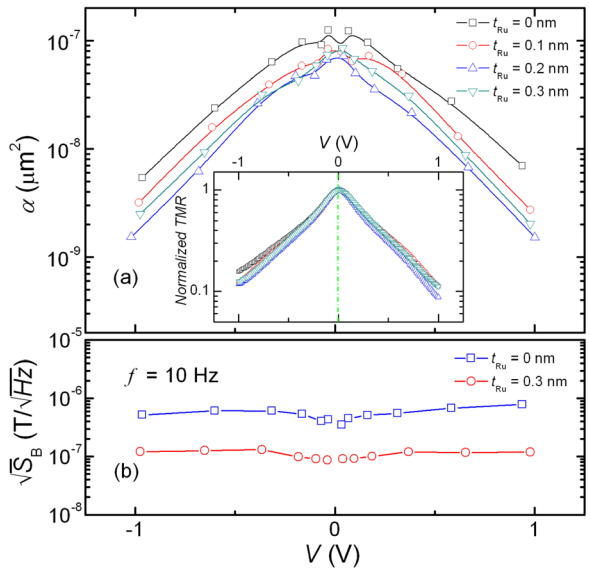

FIG. 4. (a) Hooge-like parameter α during magnetization switching of the top pinned layer as a function of bias voltage for different t_{Ru}, the inset gives the normalized TMR (V) curves. (b) The bias dependence of field detectivity level both for $t_{Ru} = 0$ and 0.3 nm.

normalized by a Hooge-like parameter $\alpha = AfS_v/V^2$, where A is the junction area, f is the frequency, S_v is the noise power spectral density, and V is bias voltage.[18–21] The noise peaks in Figure 3(a) are consistent with magnetization rotation of the two ferromagnetic layers. One narrow peak around zero field belongs to the magnetization rotation of the top-pinned CoFeB, and the other around +50 mT is from the bottom-pinned CoFeB. Obviously, the noise level of the ferromagnetic layers in the antiparallel state is much higher compared to that in the parallel state due to the magnetic fluctuation contribution.[13,30] In a field of −400 mT, the device is almost in the parallel state, but the noise magnitude increases on increasing the field, which is related to the spin flop configuration adapted by the SAF in a range of field around −200 mT.[22,23] As shown in Fig. 1(b), the magnetization of the lower pinned layer is properly saturated when the magnetic field changes from −400 to −50 mT. The noise level continues to increase and shows a bump shape in this field range. This is different from ordinary MTJs, where the noise level is almost independent of field in the range from −200 to −50 mT.[13,24]

Usually, equilibrium magnetic $1/f$ noise exhibits a linear dependence on the field sensitivity range[25,26] $(1/\mu_0 R)(\mathrm{d}R/\mathrm{d}H)$. The linear response plotted in Fig. 3(b) further confirms that the noise during the magnetization switching for our sensors is equilibrium noise of magnetic origin. The sensor's equilibrium $1/f$ field noise in units of T^2/Hz can be determined from[7,26]

$$S_B = \frac{\alpha}{Af}\left(\frac{1}{\mu_0 R}\frac{dR}{dH}\right)^{-2}. \quad (1)$$

Using data from Fig. 3(b), the field detectivity of our sensors, $\sqrt{S_B}$, at 1 Hz is about 280 nT/$\sqrt{Hz}$ with $t_{Ru} = 0.3$ nm. It further decreases to ~90 nT/$\sqrt{Hz}$ at 10 Hz, which is comparable with the field detectivity of other types of MR sensor.[7,20,27] Moreover, the detectivity decreases greatly after inserting the thin Ru layer (Fig. 4(b)). A better noise detectivity has been reported only for MTJ sensors with a thinner free layer or with field bias, which gives a very limited field range.[10,28,29]

Figure 4(a) and the inset show the bias dependence of α during magnetization switching of the top pinned layers and the normalized TMR. By inserting the thin Ru layer, the bias dependence of both the noise and TMR becomes more symmetric. Below 100 mV, α is roughly constant during the magnetization switching, which is similar to that in ordinary MgO-MTJs.[30,31] At high bias, the noise during magnetization switching of the top-pinned electrode is strongly bias dependent. Lower noise level can be obtained under higher bias. However, the field detectivity level increases a little with bias, as shown in Fig. 4(b), which is consistent with the results in Ref. 29. The trend for the bias dependence of noise in Fig. 4(a) is similar to that of TMR. This can be attributed to the variation of junction resistance with bias voltage.[30,31]

In conclusion, a fully functional TMR sensor based on MgO-barrier MTJs with pinned bottom and top CoFeB layers has been demonstrated. The thin Ru layer inserted between the top CoFeB and IrMn permits systematic tuning of the exchange coupling, the linear TMR field range, and the sensitivity. When the TMR ratio exceeds 200%, the field sensitivity can be as high as 26%/mT and field detectivity as low as 90 nT/$\sqrt{Hz}$ at 10 Hz. The tunability of this type of MTJ sensor with a wide field range is independent of the shape of device, which could be beneficial for scalable magnetic sensor applications.

The authors thank H. Kurt and R. Stearrett for helpful discussions, M. Venkatesan for the SQUID measurement.

The work was supported by the EU as part of FP7 NAMDIATREAM Project and by Science Foundation Ireland as part of the Nanoscale Interface and Spin Electronics (NISE) Project (10/IN1/I3002).

[1]W. H. Butler, X.-G. Zhang, T. C. Schulthess, and J. M. MacLaren, Phys. Rev. B **63**, 054416 (2001).
[2]J. Mathon and A. Umersky, Phys. Rev. B **63**, 220403 (2001).
[3]S. S. P. Parkin, C. Kaiser, A. Panchula, P. M. Rice, B. Hughes, M. Samant, and S. H. Yang, Nat. Mater. **3**, 862 (2004).
[4]S. Yuasa, A. Fukushima, T. Nagahama, K. Ando, and Y. Suzuki, Nat. Mater. **3**, 868 (2004).
[5]S. Ikeda, J. Hayakawa, Y. Ashizawa, Y. M. Lee, K. Miura, H. Hasegawa, M. Tsunoda, F. Matsukura, and H. Ohno, Appl. Phys. Lett. **93**, 082508 (2008).
[6]W. J. Gallagher and S. S. P. Parkin, IBM J. Res. Dev. **50**, 5 (2006).
[7]P. P. Freitas, R. Ferreira, S. Cardoso, and F. Cardoso, J. Phys.: Condens. Matter **19**, 165221 (2007).
[8]S. Matsunaga, J. Hayakawa, S. Ikeda, K. Miura, H. Hasegawa, T. Endoh, H. Ohno, and T. Hanyu, Appl. Phys. Exp. **1**, 091301 (2008).
[9]C. Albon, A. Weddemann, A. Auge, K. Rott, and A. Hutten, Appl. Phys. Lett. **95**, 023101 (2009).
[10]J. M. Almeida, R. Ferreira, P. P. Freitas, J. Langer, B. Ocker, and W. Maass, J. Appl. Phys. **99**, 08B314 (2006).
[11]B. Negulescu, D. Lacour, F. Montaigne, A. Gerken, J. Paul, V. Spetter, J. Marien, C. Duret, and M. Hehn, Appl. Phys. Lett. **95**, 112502 (2009).
[12]A. J. Devasahayam and M. H. Kryder, J. Appl. Phys. **85**, 5519 (1999).
[13]G. Q. Yu, Z. Diao, J. F. Feng, H. Kurt, X. F. Han, and J. M. D. Coey, Appl. Phys. Lett. **98**, 112504 (2011).
[14]S. Yuasa, and D. D. D. Djayaprawira, J. Phys. D: Appl. Phys. **40**, R337 (2007).
[15]T. Ibusuki, T. Miyajima, S. Umehara, S. Eguchi, and M. Sato, Appl. Phys. Lett. **94**, 062509 (2009).
[16]P. W. T. Pong and W. F. Egelhoff, J. Appl. Phys. **105**, 07C915 (2009).
[17]G. Malinowski, M. Hehn, M. Sajieddine, F. Montaigne, E. Jouguelet, F. Canet, M. Alnot, D. Lacour, and A. Schuhl, Appl. Phys. Lett. **83**, 4372 (2003).
[18]E. R. Nowak, M. B. Weissman, and S. S. P. Parkin, Appl. Phys. Lett. **74**, 600 (1999).
[19]L. Jiang, E. R. Nowak, P. E. Scott, J. Johnson, J. M. Slaugher, J. J. Sun, and R. W. Dave, Phys. Rev. B **69**, 054407 (2004).
[20]C. Ren, X. Y. Liu, B. D. Schrag, and G. Xiao, Phys. Rev. B **69**, 104405 (2004).
[21]J. Scola, H. Polovy, C. Fermon, M. Pannetier-Lecoeur, G. Feng, K. Fahy, and J. M. D. Coey, Appl. Phys. Lett. **90**, 252501 (2007).
[22]R. S. Beach, J. McCord, P. Webb, and D. Mauri, Appl. Phys. Lett. **80**, 4576 (2002).
[23]B. Negulescu, D. Lacour, M. Hehn, A. Gerken, J. Paul, and C. Duret, J. Appl. Phys. **109**, 103911 (2011).
[24]R. Stearrett, W. G. Wang, L. R. Shah, A. Gokce, J. Q. Xiao, and E. R. Nowak, J. Appl. Phys. **107**, 064502 (2010).
[25]Z. Diao, E. R. Nowak, K. M. Haughey, and J. M. D. Coey, Phys. Rev. B **84**, 094412 (2011).
[26]A. Ozbay, A. Gokce, T. Flanagan, R. A. Stearrett, E. R. Nowak, and C. Nordman, Appl. Phys. Lett. **94**, 202506 (2009).
[27]D. Mazumdar, X. Y. Liu, B. D. Schrag, W. F. Shen, M. Carter, and G. Xiao, J. Appl. Phys. **101**, 09B502 (2007).
[28]R. C. Chaves, P. P. Freitas, B. Ocker, and W. Maass, J. Appl. Phys. **103**, 07E931 (2008).
[29]J. M. Almeida, P. Wisniowski, and P. P. Freitas, J. Appl. Phys. **103**, 07E922 (2008).
[30]Z. Diao, J. F. Feng, H. Kurt, G. Feng, and J. M. D. Coey, Appl. Phys. Lett. **96**, 202506 (2010).
[31]J. M. Almeida, P. Wisniowski, and P. P. Freitas, IEEE Trans. Magn. **44**, 2569 (2008).